Demand Response of Medical Freezers in a Business Park Microgrid

Rosa Morales González[1], Madeleine Gibescu[1], Sjef Cobben[1,2],
Martijn Bongaerts[2], Marcel de Nes-Koedam[2] and Wouter Vermeiden[2]
[1]*Electrical Energy Systems Group, Department of Electrical Engineering, Eindhoven University of Technology, 5612AP Eindhoven, The Netherlands*
[2]*Alliander N.V., 6812AH Arnhem, The Netherlands*

Keywords: Demand Response, Genetic Algorithm, Local RES Integration, Physical System Modeling, Smart Grid.

Abstract: This paper presents a demand response (DR) framework that utilizes the flexibility inherent to the thermodynamic behavior of four groups of independently-controlled medical freezers in a privately-owned business park microgrid that contains rooftop photovoltaics (PV). The optimization objectives may be chosen from the following 3 options: minimizing electricity exchanges with the public grid; minimizing costs by considering prices and RES availability; and minimizing peak load. The proposed DR framework combines thermodynamic models with automated, genetic-algorithm-based optimization, resulting in demonstrable benefits in terms of cost, energy efficiency, and peak power reduction for the consumer, local energy producer, and grid operator. The resulting optimal DR schedules of the freezers are compared against unoptimized, business-as-usual scenarios with- and without PV. Results show that flexibility can be harnessed from the thermal mass of the freezers and their contents, improving the cost- and energy performance of the system with respect to the business-as-usual scenarios.

1 INTRODUCTION

Increasing distributed generation from renewable energy sources (DG-RES), such as solar and wind, into electricity networks poses several challenges due to the resources' stochastic nature (Hewicker et al., 2012). This variability brings about a loss of flexibility in the generation side of the power system value chain, since the electricity generation profile can no longer ramp up or down to adapt to the load profile. Within the evolution of power systems, the concept of *smart grids* proposes different technical solutions that can harness flexibility from other sources to compensate for the loss of flexibility from the generation side: e.g., enhanced monitoring and control functionalities, electrical and/or thermal storage, novel electricity market designs, and increased demand-side flexibility through demand response (DR) programs (Huber et al., 2014; Alizadeh et al., 2016). Demand response is defined as the set of "actions voluntarily taken by consumers [and/or prosumers] to change their energy usage —either in terms of quantity or timing— in response to an external control signal" (Morales González et al., 2016), e.g., price or a direct command from the aggregator or system operator.

Thermostatically-controlled loads have become a valuable flexible resource of DR programs in the residential sector, where water heaters (Gelažanskas and Gamage, 2016), refrigerators (Liu et al., 2014), and HVAC systems (Yoon et al., 2014) have been targeted for the implementation of DR programs in the residential sector. However, in order to unlock their full potential, the (small) loads have to be aggregated in large numbers. This is not always possible in pilot programs involving residential consumers, due to low participation of the customer base, limited resources and large investment requirements, as discussed in (He et al., 2013; Klaassen et al., 2014; D'hulst et al., 2015; Labeeuw et al., 2015).

Commercial and industrial (C&I) consumers, on the other hand, have an overall higher consumption footprint and a higher peak demand (European Environment Agency, 2017). Furthermore, C&I consumers are usually located in concentrated areas such as business/industrial parks, which facilitates aggregation and makes this type of end-users interesting for applying DR programs (Ashok and Banerjee, 2000; Grünewald and Torriti, 2013). Several strategies have been proposed for different types of heavy industry

Morales González, R., Gibescu, M., Cobben, S., Bongaerts, M., de Nes-Koedam, M. and Vermeiden, W.
Demand Response of Medical Freezers in a Business Park Microgrid.
DOI: 10.5220/0006801001200129
In *Proceedings of the 7th International Conference on Smart Cities and Green ICT Systems (SMARTGREENS 2018)*, pages 120-129
ISBN: 978-989-758-292-9
Copyright © 2019 by SCITEPRESS – Science and Technology Publications, Lda. All rights reserved

in works such as (Matthews and Craig, 2013; Mitra et al., 2013; Finn and Fitzpatrick, 2014), but DR is still not implemented systematically in this sector because industrial consumers' energy needs vary greatly from one another and applications for DR can be restricted in scope due to the nature or sensitivity to changes of the processes inherent to the industry (Samad and Kiliccote, 2012; Ton and Smith, 2012).

Authors such as the ones from (Zavala, 2013; Ma et al., 2015; Yin et al., 2016; Hurtado et al., 2017) have written extensively on the flexibility of commercial buildings in cities through buildings' passive thermal capacitance and HVAC controls. Their findings on the DR potential of commercial buildings are especially relevant to the case of the Netherlands, where the service industry is the second largest energy consumer behind heavy industry (Centraal Bureau voor de Statistiek, 2017a). This sector has seen steady and rapid growth in the past twenty years and contributes to the highest added value and employment in the Dutch economy (Compendium voor de Leefomgeving, 2017).

In this work, we focus on the DR potential of the health services sector, ranked in the top three sectors of the Dutch economy (Centraal Bureau voor de Statistiek, 2017b). We propose and test a DR framework with a case study of a business park microgrid with local PV generation in which the flexible load is a medical freezing warehouse. Freezer loads are shifted in time by automated DR actions, controlling the medical freezers in four independent clusters, while treating PV production as a curtailable/reparameterizable resource. The case study evaluates the benefits of the DR program over a 48-hour time window with a resolution of 15-minutes. We study a 48-hour optimization window in order to observe the temperature dynamics of the freezers on a longer term than day-ahead, and to solve a more complex problem that can test the robustness of our framework.

Our main contributions are the iterative embedding of the thermodynamic freezer model into an optimization algorithm to form a single DR framework, and its application to a real-world situation. This work explores 1) how flexibility can be harnessed from the freezer contents' thermal mass, and 2) what the resulting benefits are in terms of cost, energy efficiency and peak load reduction for the consumer, the local DG-RES producer, and the operator of the business park microgrid.

The rest of the paper is organized as follows: Section 2 describes the mathematical models, and Section 3 describes the case study used for this work. In Sections 4 and 5, results are presented and discussed. Finally, conclusions and directions for future work are stated in Section 6.

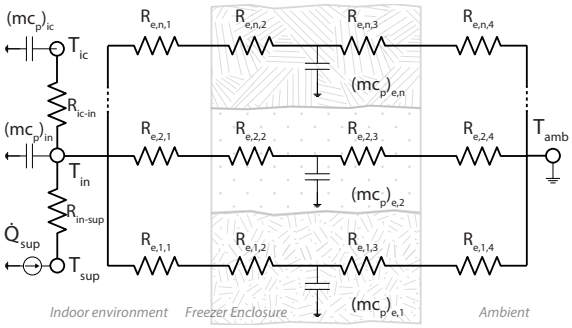

Figure 1: Equivalent RC circuit of the medical freezers.

2 METHODOLOGY

This section describes the mathematical models and algorithms that make up the physical models, in combination with our optimization-based DR framework.

2.1 Thermodynamic Modeling

The thermodynamics of the medical freezers in the research facility can be described by a first-order dynamic system, as described in works such as (Zaparoli and de Lemos, 1996; Lampropoulos et al., 2013; Kalsi et al., 2011; Hurtado et al., 2015; Wilson et al., 2015). The generic, lumped parameter resistance/capacitance (RC) circuit model, shown in Figure 1, is used to achieve a better understanding of how the thermal mass of buildings can unlock demand-side flexibility in terms of available shifting power and duration and possible energy/cost savings. This simplified representation of end-user premises allows us to 1) capture first-order transients without having to perform a heavily-detailed simulation, and 2) facilitate the real-time implementation of the optimization framework we use in our DR program. The system of equations describing the thermodynamic behavior of the medical freezers is given in equation (1):

$$(mc_p)_{ic} dT_{ic}(t)/dt = -(T_{ic} - T_{in})/R_{ic-in} \tag{1a}$$

$$(mc_p)_{in} \frac{dT_{in}(t)}{dt} = \frac{T_{ic} - T_{in}}{R_{ic-in}} - \frac{T_{in} - T_{sup}}{R_{in-sup}} - \sum_{n=1}^{N} \frac{T_{in} - T_{e,n}}{R_{e,n,1} + R_{e,n,2}} \tag{1b}$$

$$(mc_p)_{e,n} \frac{dT_{e,n}(t)}{dt} = \frac{T_{in} - T_{e,n}}{R_{e,n,1} + R_{e,n,2}} - \frac{T_{e,n} - T_{amb}}{R_{e,n,3} + R_{e,n,4}} \quad \forall n \in [1, N] \tag{1c}$$

$$0 = (T_{in} - T_{sup})/R_{conv} + \dot{Q}_{sup} \tag{1d}$$

where $(mc_p)_x$ denotes heat capacity in J/K; $dT_x(t)/dt$, is the rate of change temperature with respect to time in K/s; and R_x denotes thermal resistance in K/W. The subscript x is a stand-in for the subscripts ic, in, sup and e, n, (see corresponding blocks in Figure 1) which denote the freezer's interior contents, indoor air, heat supply system (evaporator coil), and n number of enclosure elements out of a total N (e.g., freezer roof, walls, floor), respectively. T_{amb} is the ambient temperature (i.e. temperature of the conditioned space in which the freezers are kept) as a function of time in degrees Kelvin (K), $\dot{Q}_{sup}$ is the heat extracted by the freezer's mechanical cooling system in watts, and T_{sup} is the supply temperature of the mechanical cooling system in K.

Mechanical heat extracted is related to electrical power consumption, $\dot{W}_{el}$, through the coefficient of performance (COP) of the freezers' mechanical cooling system, defined by (2):

$$COP = \dot{Q}_{sup}/\dot{W}_{el} \tag{2}$$

Assuming that the conditioned space in which the freezers are kept is maintained at a constant temperature to ensure the optimal operation of the mechanical refrigeration system, we may assume a constant COP; hence, mechanical heat extracted is given by (3):

$$\dot{Q}_{sup} = COP \times \dot{W}_{el} \tag{3}$$

Finally, assuming we can independently control the operation of the medical freezer in i clusters, the electricity consumption of each cluster at time t is given by (4):

$$E(i,t) = \int_{t-1}^{t} \dot{W}_{el}(i,t)dt \tag{4}$$

2.2 Optimization Problem Formulation

Let us consider that the ON/OFF signal of the medical freezers of cluster i at time t is defined by the binary variable $\beta(i,t)$. The net energy imported from the grid of all I freezers at the research facility, $E_{net}(t)$, after combining the predicted contribution of local DG-RES in the microgrid $E_{RES}(t)$ and the electricity consumption of the independently-controlled freezer clusters i at time t, $E(i,t)$, is expressed by (5):

$$E_{net}(t) = \sum_{i=1}^{I} \beta(i,t)E(i,t) - E_{RES}(t) \tag{5}$$

The optimization problem (6a) signifies choosing the ON/OFF switching schedules ($\beta(i,t)$) and the PV production schedule $E_{RES}(t)$ over the whole time horizon, with the objective of minimizing energy exchanges with the regional grid (7), peak power consumption (8), or overall energy cost (12). Each of these optimization problems is analyzed separately. The freezer temperatures ($T_{in}(i,t)$) must not exceed the critical values required by the end-users (6b). Physical constraints of local DG-RES production (6c) are considered. Finally, the rated capacity of the connection, P_{max}, should not be exceeded (6d). The optimization problem takes on the form (6):

$$\min_{\beta, E_{RES}} \quad \Omega = \Phi \tag{6a}$$

$$\text{s.t.} \quad T_{min}(i,t) \le T_{in}(i,t) \le T_{max}(i,t) \quad \forall i,t \tag{6b}$$

$$0 \le E_{RES}(t) \le E_{RES}^{max}(t) \quad \forall t \tag{6c}$$

$$|P_{net}| \le P_{max} \tag{6d}$$

with $P_{net}(t) = \sum_{i=1}^{I} \beta(i,t)\dot{W}_{el}(i,t) - P_{RES}(t)$. Φ stands in for Φ_e (7) in the energy consumption minimization-, Φ_p (8) in the peak load reduction- , and Φ_c (12) in the energy cost minimization problem variants:

$$\Phi = \Phi_e = \sum_{t=1}^{T} |E_{net}(t)| \tag{7}$$

$$\Phi = \Phi_p = max(|P_{net}|) \tag{8}$$

For the cost optimization problem, let λ_{RES} be the price per kilowatt-hour the local consumer pays for buying locally-produced energy in the microgrid, λ_{grid} the price for buying electricity from the regional electricity supplier, and λ_{feedin} the tariff the local DG-RES producer gets for exporting PV to the regional distribution network. Let us assume that the DG-RES producer sells its electricity at a lower price than the consumer would pay for electricity from the regional electricity supplier, and that the feed-in tariff it gets for feeding the electricity back into the regional network is considerably less than that it receives for selling electricity locally within the microgrid (9):

$$\lambda_{feedin} \ll \lambda_{RES}(t) < \lambda_{grid}(t) \quad \forall t \tag{9}$$

The total cost for the consumer is given by (10):

$$\sum_{t=1}^{T} (\lambda_{RES}(t)E_{RES}(t) + \lambda_{grid}(t)E_{imports}(t)) \tag{10}$$

where $E_{RES}(t)$ is energy consumed from local DG-RES, and $E_{imports}(t)$ is energy consumed from grid imports in the microgrid —i.e., when $E_{net} > 0$— at time t. The total revenue for the DG-RES producer from feeding in energy back into the grid —i.e., when $E_{net} > 0$— is denoted $E_{exports}(t)$ and defined as (11):

$$\sum_{t=1}^{T} (\lambda_{RES}(t)E_{RES}(t) + \lambda_{feedin}(t)E_{exports}(t)) \tag{11}$$

Maximizing producer revenue and minimizing consumer costs, we have:

$$\Phi = \Phi_c = \sum_{t=1}^{T} (\lambda_{grid}(t) E_{imports}(t) - \lambda_{feedin}(t) E_{exports}(t)) \quad (12)$$

Constraint (6b) determines the flexibility of the freezer and enforces the critical temperature ranges for each freezer cluster i: $T_{min}(i,t)$ and $T_{max}(i,t)$. The values of $T_{in}(i,t)$ are obtained from the thermodynamic freezer submodels. Constraint (6c) enforces the physical upper and lower bounds of local DG-RES production. The resulting non-linear, mixed-integer optimization problem is too complex to be solved by traditional methods in reasonable time. From the family of heuristic search techniques, we opted for the genetic algorithm (GA) for its ability to efficiently deal with both continuous and discrete decision variables.

2.3 Interaction Between Models

While conventional freezer temperature controls have a fixed set-point temperature and fixed temperature trip points based on indoor air temperature measurements, our multiphysics DR framework couples and iteratively intertwines the thermodynamic freezer models with the GA-based optimization framework to: 1) calculate temperature limits based on the freezer contents instead of the indoor air to gain extra flexibility from the products' inherent thermal mass; and 2) to devise optimal on/off strategies for all freezer clusters in the building, such that the objectives of minimal cost, maximal energy self-sufficiency or minimum peak load are achieved. Note that the optimization problem will determine the entire 48-hour switching schedule in advance of real-time, assuming perfect knowledge and/or accurate forecasts of all influencing factors: feed-in tarrifs, wholesale and local market prices, and short-term PV production.

3 CASE STUDY

This section describes the case study for which the simulation experiments were performed, as well as all relevant technical characteristics.

Our DR framework is applied to a freezing warehouse used for medical research in the Netherlands. The medical freezing facility is located in a business park that operates as a local, private microgrid interconnected to the regional grid via a consumer substation. Grid constraints are not an issue in this case, since all network assets have been overdimensioned. A 250-kWp photovoltaic installation consisting of 1700 m^2 of crystalline PV panels is also coupled to the business park microgrid through the consumer substation. The PV modules are made of crystalline silicone, and have a 15% efficiency. The energy conversion efficiency of the PV modules is 80%. Overall, the PV system efficiency is thus 12%. Electricity generated locally by the PV installation is 157 MWh/y. The medical freezing facility consumes approximately 1.4 GWh/y. It stores blood samples at a temperature of -80°C in 120 freezer units. The freezer units consume approximately 500 MWh/y in total, representing 35% of the total energy consumption in the medical freezing facility.

The blood samples are preserved in a glycerol solution for long-term storage. In setting our flexibility thresholds for the freezer temperatures, we refer to industry best practices. These dictate that the temperature of the glycerolized red blood cells during storage should not exceed -60°C in order to avoid the deterioration of the samples (Maharashtra State Blood Transfusion Council, 2014; Eftekhar, 1989; Wessling and Blackshear, 1973). We set a conservative flexibility temperature upper limit of -70°C to remain well within the limits for sample quality preservation. The temperature of the blood samples, (i.e., the temperature of the freezers' internal contents, T_{ic} in Figure 1 and eq. (1) will be used for the constraints formulation of the optimization problem. This means that T_{ic} will be allowed to oscillate between -80 and -70°C with a tolerance of $\pm$0.3°C to account for system delay in our GA-based controller.

The density and specific heat capacity of glycerolized red blood cells for the freezer working temperatures are compiled from (Eftekhar, 1989; Wessling and Blackshear, 1973), and are shown in Table 1, and compared against values for whole blood, as a reference. The values for glycerolized red blood cells will be used in our DR framework's building models to represent the internal contents of the medical freezers.

In this work, we assume that 1) the internal contents of the freezer are already "at temperature", and 2) there is no in- or outflow of samples during the 48h time horizon of the DR optimization problem. In other words, the mechanical refrigeration system of the freezers are only used to maintain the product temperature. We contend this is a reasonable assumption given that the medical freezing warehouse is a long-term research facility in which samples are kept in storage in the order of years, even decades.

In our energy calculations for the medical research freezing facility, we neglect the base electricity load

Table 1: Thermophysical properties of blood components.

Blood component	ρ [kg/m^3]	c_p [kJ/(kgK)]
Glycerolized red blood cells	1063	1.5
Whole blood	980	3.6

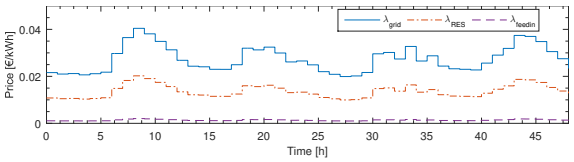

Figure 2: Dynamic electricity prices for the end-users of the microgrid.

and any loads triggered by human interaction. Heating or cooling loads required to balance ventilation and internal heat gains/losses from lighting, people, and equipment could be additional sources of flexibility in the building, but are not taken into consideration in the present case study.

We assume that all end-users are subjected to the same hourly electricity prices; and that electricity prices and PV generation for the optimization horizon can be forecasted with a reasonable degree of accuracy. Expected day-ahead electricity prices[1] and PV generation values for average irradiation days[2] used in the simulations are shown in Figure 2 and Figure 3.

Three optimization objectives are considered separately: 1) energy minimization (i.e., reducing energy exchanges with the regional grid), 2) cost minimization, and 3) peak load minimization. The optimization results are compared against a Business-As-Usual (BAU) scenario, where temperature control in the freezers is driven by their conventional, continuously-operating thermostats with a fixed setpoint and deadband. We compare results of switching all 120 freezers at the same time in the BAU scenario (worst-case scenario for peak load) against having four clusters of 30 freezers each that can be independently controlled. Because grid constraints are not an issue in the present case study, we set P_{max} to the worst-case scenario for peak load, or 132 kW, in constraint (6d).

The design variables of the optimization problem are the 15-minute switching schedules of the mechanical refrigeration system for all freezer clusters, binary variable $\beta(i,t)$, and the 15-minute DG-RES production schedules, $E_{RES}(t)$. E_{RES} is a continuous non-negative variable on the interval [0,1] based on the maximum forecasted production for that 48-hour time horizon. For the 48-hour time window of the case study, β has a length of 193 elements per i cluster of freezers, and the microgrid-aggregated E_{RES} has a length of 193, resulting in a phenotype of 965 elements. Results were obtained by parallelizing the GA computations into twenty-eight pools of workers using MATLAB's Parallel Computing Toolbox. The simulations were carried out using an Intel Xeon CPU with two processors running at 2.6 GHz.

[1]Based on data from https://transparency.entsoe.eu/

[2]Based on data from http://www.soda-pro.com/web-services#radiation

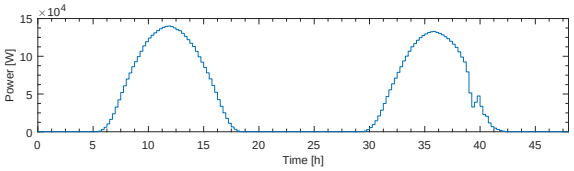

Figure 3: PV production profiles for two consecutive average solar irradiation days in the Netherlands (1700m^2, system efficiency 12%).

3.1 Freezer Model

Each of the ultra-low temperature freezers used in the medical research facility have a rated capacity of 1.1 kW and a COP of 0.575 at $T_{amb} = 25°C$. Their electricity consumption under no-load conditions —i.e., with an empty freezer— at a setpoint of -80 °C is 11.5 kWh/day. The peak load when all freezers are on at the same time is 132 kW.

The freezers' external and internal dimensions are $1030 \times 882 \times 1993$ mm and $870 \times 600 \times 1400$ mm, respectively. The freezer enclosures are 80 mm-thick, and consist of vacuum-insulated panels sandwiched between painted AISI type 304 stainless steel sheets, which are commonly used in the manufacturing of cryogenic vessels and refrigeration equipment. Thermophysical properties of the freezer enclosure were calculated with data from (ASM Aerospace Specification Metals Inc., ; MatWeb, 2017), and are given in Table 2.

The heat transfer mechanisms we consider in the freezer model are conduction and convection. The low emissivity values of the freezer enclosure materials make the magnitude of radiative heat transfer negligible compared to the magnitudes of the conductive heat transfer from the evaporator coils to the inner chamber of the freezer, and the convective heat transfer due to the forced air distribution system inside the freezer chamber.

The internal volume of each freezer is 729 liters, which can fit 576 vial storage boxes, each containing one hundred 1-ml samples. This means that the total volume of blood samples contained in each freezer is 57.6 liters, or approximately 8% of the total volume of the freezer chamber.

Table 2: Thermophysical properties of the freezer enclosure.

	Value	Unit
Thermal conductivity, k	0.01	W/(mK)
Heat transfer coefficient, h	8	W/(m^{2}K)
Specific heat capacity, c_p	650	J/(kgK)
Density, ρ	186	kg/m^3

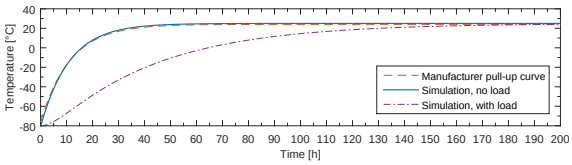

Figure 4: Pull-up system response comparison.

3.2 Freezer Model Validation

In order to validate our model, we compared a simulation of the freezer response without any load nor contributions from the refrigeration system with the freezer pull-up curve from the manufacturer. The system response simulation in Figure 4 is shown in a solid blue line against the manufacturer data, plotted as a dashed red line. There is a very good match between the manufacturer data and simulation results, which means that the model is sufficiently accurate for our purposes. The figure shows that the time constant of the system is approximately 70 hours with an empty freezer. Our results are also in the same order of magnitude, but comparatively higher than those in refrigerators for residential applications, where a time constant of approximately 20-30 hours is found (Verzijlbergh and Lukszo, 2013). Figure 4 also compares the pull-up system response under no-load conditions (solid blue line) against the fully-loaded freezer with blood samples described in the previous subsection (purple dash-dotted line). It can be seen from the figure that the time constant of the system increases almost threefold, going from 70 hours in the no-load case to 200 hours in the fully-loaded case, which is as expected.

We also simulated the performance of the freezer under no-load conditions and compared it against the electricity consumption given by the manufacturer. Simulation results under no-load conditions show that the daily electricity consumption of the freezer is 12.4 kWh/day. This represents a 7% error difference, but is nevertheless a good, if conservative, approximation of the freezer's cooling capacity that will take into account future degradation of the freezer's mechanical refrigeration system that comes with normal use.

4 RESULTS

This section presents the simulation results for the BAU scenario, plus the energy amount, energy cost, and peak reduction optimizations. Due to the heuristic nature of the GA, a number of local minima were found in successive runs, and the best results are reported graphically in Figs. 5-8, and are summarized and compared against each other in Table 3.

4.1 BAU Scenario

Simulation results for the BAU scenario are shown in Figure 5, which contains three subplots. The topmost subplot (a) shows freezer contents (blue solid line) and indoor temperatures (red solid line) with respect to time. The middle subplot (b) shows whether the mechanical refrigeration system is switched on at every time step. Finally, the bottom subplot (c) shows the electrical power consumption with respect to time in a scenario with local PV generation, with positive values denoting consumption and negative values denoting generation.

Results show that local PV generation by itself has a beneficial effect on cost and energy reduction. However, it is possible to see from Figure 5(c) and Table 3 that an uncontrolled PV production has an adverse effect in the system, in the form of a 5% increase in the peak load from 132 to 139 kW.

4.2 Optimization Results

Optimization results are shown in Figure 6, Figure 7 and Figure 8 for the energy, cost, peak power minimization objectives, respectively. The subplots and legends for all optimization results are analogous to those of Figure 5. In subplot (a), Ti_{blood} denotes the temperature of the blood samples of cluster i of independently controllable freezers. The DR scheduling process took approximately one and a half hours to converge for each run in the MATLAB/Simulink simulation environment.

The energy minimization objective is apparent in Figure 6(b), since net energy exchanges with the electricity grid during times of solar energy production are kept as close to zero as possible. The ability to reduce the cooling load without infringing upon the thermal safety boundaries is due to the freezers' thermal mass; i.e., the summation of the heat capacities of the different freezer enclosure elements and their contents: term $(mc_p)_x$ in (1). Because of this need to keep grid imports and exports to a minimum, the PV utilization rate goes down to 77% with respect to the uncontrolled BAU scenario with PV. Energy and cost

Table 3: Optimization results vs BAU scenario.

Scenario	Energy [kWh]			[€]	[%]			
	Imports	Exports	Total exchange	Social cost	Cost savings	Energy savings	Peak reduction	PV utilization
BAU, no PV	3369.3	0	3369.3	92.89	—	—	—	0
BAU + PV, no DR	2235.1	793.2	3028.3	59.15	36	10	-5	100
Energy optimization	1482.1	35.1	1517.2	40.11	57	55	0	77
Cost optimization	1423.8	280.6	1704.4	36.92	60	49	0	88
Peak load optimization	2158.7	138.5	2297.2	58.37	37	32	25	50

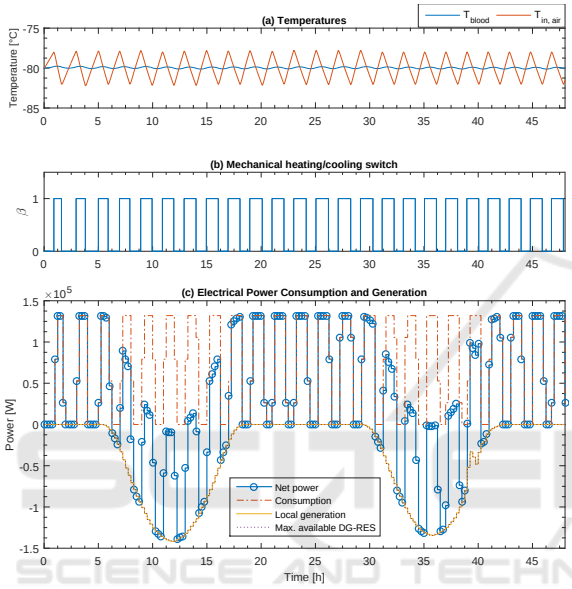

Figure 5: Results for the BAU scenario + DG-RES, no DR.

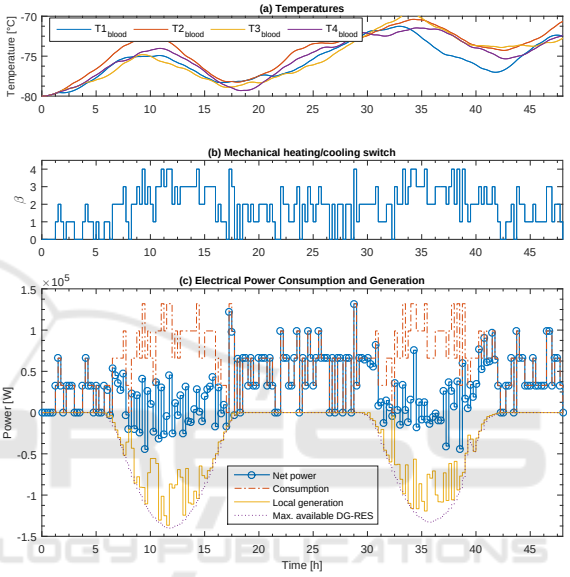

Figure 6: Results for energy minimization.

savings are 55% and 57% respectively; however, this optimization objective does not have any noticeable effect on peak reduction.

From Table 3, although net energy consumption is higher in the cost optimization scenario, cost performance slightly improves, signifying a reduction of 60% with respect to the BAU scenario. Results in Figure 7(c) show that consumption concentrates not only on the times where the electricity prices are low, but also where PV production is highest. As can be seen in Table 3, the PV utilization rate is 12% less than in the BAU case with uncontrolled PV generation and no DR.

The peak power minimization objective does precisely what it is supposed to do, keeping at most three freezer clusters on at the same time or having all four clusters on at times where PV is being produced to keep peak power as low as possible. This scenario had the lowest energy and cost savings performance of the three optimization objectives studied in this work. However, the results obtained for the peak minimiza-

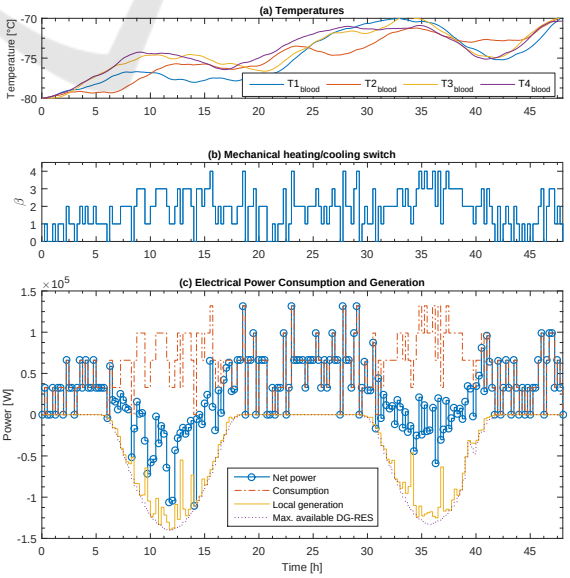

Figure 7: Results for cost minimization.

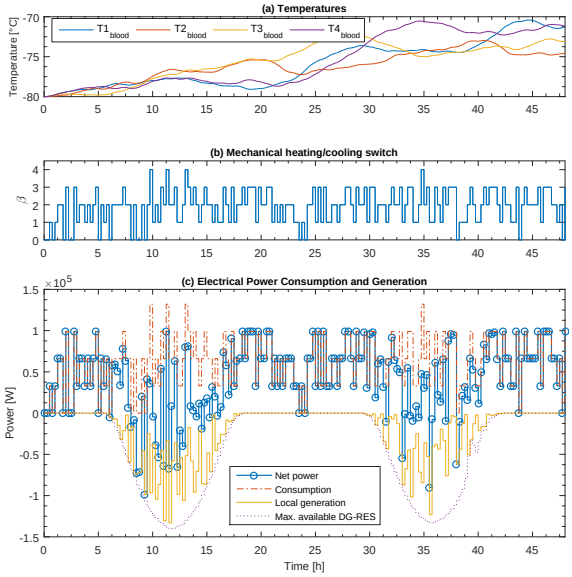

Figure 8: Results for peak minimization.

tion objective still outperform those for the BAU with uncontrolled PV scenario, with the added benefit of reducing net peak power by 25%: a benefit that is extended not only for the microgrid consumers' capacity connection fees but also to the network operator, as network reinforcements due to increased loads can be delayed (although in this case study it is not a critical problem).

Figure 9 shows the distribution of fitness function values from all the successive simulation runs for each optimization variant. They are expressed as the difference with respect to the results from the BAU scenario. Mean values for the simulation successions performed for this work were $(46 \pm 8)\%$ for the energy-, $(56 \pm 2)\%$ for the cost minimization, and $(21 \pm 6)\%$ for the peak reduction variants.

5 DISCUSSION

The results presented in the previous section show the potential of implementing both price-responsive (cost minimization) and direct control (peak load minimization) DR programs to harness flexibility from C&I customers' thermostatic loads. The benefits of harnessing this flexibility are clear and attractive, in terms of reductions in the amount and overall cost of electricity demand for the end-users connected to the microgrid. In the case of peak load reduction, possible deferrals in network reinforcement investments and/or lower connection costs are also present. This assertion holds for comparisons against both the BAU scenario with no DG-RES and the BAU scenario with

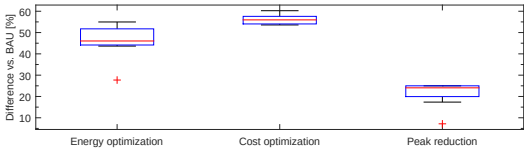

Figure 9: Distribution of fitness function values for each optimization variant.

DG-RES but no demand response. The benefits of combining DR with customer thermostatic loads and local DG-RES available in the microgrid is especially evident when comparing results in terms of peak load mitigation with respect to the BAU scenario with uncontrolled PV.

To put things in a realistic perspective, it is important to mention that the 55% energy savings in the freezers' operation translates overall to 19% energy savings in the total electricity consumption of the medical research facility. This number could be increased if, apart from the freezers, we could harness flexibility from other thermostatic loads such as heating and air conditioning systems in the rest of the medical research facility.

However, while achieving these targets, the thermal inertia of the freezers is depleted at the end of the 48-hour window, since the freezer temperatures are all at or near the temperature upper bounds of -70°C (see Figures 6(a) and 7(a)). This means that some recovery time is required immediately after the 48-hour window where DR was implemented, during which the freezers can recharge their thermal buffers (i.e., cool down to -80°C). In order to overcome this limitation, we will add end-of-horizon temperature targets in the problem formulation in future versions of this work to limit the state of charge of the thermal buffers.

Another limitation of our model is that the greater energy efficiency and lower demand/generation peaks in the C&I microgrid —while being in the interest of the microgrid as a whole— come at a loss for the local PV producer. This is because PV utilization rates become lower in the energy- and peak load minimization objectives due to PV curtailment. Since the two aforementioned optimization objectives do not take price into account, a way to increase PV utilization in these scenarios would be to add utilization constraints linked to the target payback time or return on investment for the PV producer. Similarly, in order to decrease peak load, we could include peak capacity tariffs in the objective function for the energy and cost minimization variants.

We decided to study a 48-hour window to observe the long-term temperature dynamics of the medical freezers, given the high time constant of the system. Additionally, we tested the robustness of our DR fra-

mework with this expanded time window, since the optimization problem increases in complexity given the doubled number of design variables with respect to observing a 24-hour window.

However, in practice it makes more sense to create schedules on a day-ahead basis because electricity prices would be known to the aggregator 24-hours in advance and the performance of PV production forecasting models improves the closer they are used to the period of interest. More local DG-RES can be installed in the business park if additional heating/cooling systems in the buildings located there can be harnessed in the same way we have presented in this paper without changing the network infrastructure. Scaling up or down our thermodynamic models and DR framework —depending on the size of the window, the time granularity, and the number of controllable devices— should therefore present no significant challenges when performing simulations.

Additional work is needed in order to surmount some of the assumptions made when computing the optimal schedules, especially with regards to dealing with errors in the PV forecasting data. Further steps are required in order to move out of the simulation environment and into the practical implementation of the proposed DR framework in the actual customer site, especially considering that the current convergence time is quite long. Optimizing the GA implementation in MATLAB in future versions of our work will be essential to maintain the computation time below the 24-hour window in which the DR scheduling has to be made, especially when more sources of flexibility are harnessed from the microgrid customers. Because of the non-linear, combinatorial nature of the optimization problems that make up our DR framework, the heuristic methods used to solve them require multiple successive simulation runs from which the best local optima can be selected. That is, depending on the number of flexible sources/consumers in the microgrid, it would be necessary to curtail the computation time so as not to take longer than the available scheduling window, at the expense of finding a better solution (see Figure 9).

6 CONCLUSIONS

This work modeled and optimized the thermodynamic behavior of medical freezers in a research facility in order to quantify their potential for DR programs. In summary, the results presented show that flexibility can be harnessed from the thermal mass of the freezers' enclosure and contents, resulting in significant benefits in terms of cost and energy efficiency for the end-user. Although uncontrolled DG-RES is already a significant benefit in terms of energy efficiency and cost with respect to the BAU scenario, adding DR has the following benefits: 1) reduces the coincidence of the loads, 2) improves cost and energy performance for the consumer; and 3) mitigates increased peak loads due to uncontrolled in-feed of DG-RES at the point of common coupling between the local business park microgrid and the regional distribution grid.

Future work will extend the scope of our proposed DR framework to the rest of the business park where the medical freezing warehouse is located, in order to combine the flexibility of the freezers in the medical research facility with other sources of flexibility available: other buildings and their heating/cooling systems, thermal buffers, and eventually electric vehicles.

ACKNOWLEDGMENTS

Rosa Morales González would like to thank Julian Croker for providing information on the case study, and Cees Jan Dronkers for his constructive insight on the interpretation of results.

REFERENCES

Alizadeh, M. I., Parsa Moghaddam, M., Amjady, N., Siano, P., and Sheikh-El-Eslami, M. K. (2016). Flexibility in future power systems with high renewable penetration: A review.

Ashok, S. and Banerjee, R. (2000). Load-management applications for the industrial sector. *Appl. Energy*, 66(2):105–111.

ASM Aerospace Specification Metals Inc. AISI Type 304 Stainless Steel.

Centraal Bureau voor de Statistiek (2017a). Energieverbruik; opbouw, bedrijfstak.

Centraal Bureau voor de Statistiek (2017b). Monitor topsectoren 2017.

Compendium voor de Leefomgeving (2017). Bruto toegevoegde waarde en werkgelegenheid, 1995-2016.

D'hulst, R., Labeeuw, W., Beusen, B., Claessens, S., Deconinck, G., and Vanthournout, K. (2015). Demand response flexibility and flexibility potential of residential smart appliances: Experiences from large pilot test in Belgium. *Appl. Energy*, 155:79–90.

Eftekhar, J. G. (1989). Some Thermophysical Properties of Blood Components and Coolants for D5U. Technical report, University of Texas San Antonio, San Antonio.

European Environment Agency (2017). Final energy consumption by sector and fuel.

Finn, P. and Fitzpatrick, C. (2014). Demand side management of industrial electricity consumption: Promoting

the use of renewable energy through real-time pricing. *Appl. Energy*, 113:11–21.

Gelažanskas, L. and Gamage, K. A. A. (2016). Distributed Energy Storage Using Residential Hot Water Heaters. *Energies*, 9(3):127.

Grünewald, P. and Torriti, J. (2013). Demand response from the non-domestic sector: Early UK experiences and future opportunities. *Energy Policy*, 61:423–429.

He, X., Keyaerts, N., Azevedo, I., Meeus, L., Hancher, L., and Glachant, J.-M. (2013). How to engage consumers in demand response: A contract perspective. *Util. Policy*, 27:108–122.

Hewicker, C., Hogan, M., and Mogren, A. (2012). Power Perspectives 2030: On the road to a decarbonised power sector. Technical report, Roadmap 2050, Den Haag.

Huber, M., Dimkova, D., and Hamacher, T. (2014). Integration of wind and solar power in Europe: Assessment of flexibility requirements. *Energy*, 69:236–246.

Hurtado, L., Mocanu, E., Nguyen, P., and Kling, W. (2015). Comfort-constrained demand flexibility management for building aggregations using a decentralized approach. In *SmartGreens 2015 - 4th Int. Conf. Smart Cities Green ICT Syst.*, pages 157–166, Lisbon.

Hurtado, L. A., Mocanu, E., Nguyen, P. H., Gibescu, M., and Kamphuis, I. G. (2017). Enabling cooperative behavior for building demand response based on extended joint action learning. *IEEE Trans. Ind. Informatics*, PP(99):1.

Kalsi, K., Chassin, F., and Chassin, D. (2011). Aggregated modeling of thermostatic loads in demand response: A systems and control perspective. In *Decis. Control Eur. Control Conf. (CDC-ECC), 2011 50th IEEE Conf.*, pages 15–20, Orlando. IEEE.

Klaassen, E., Frunt, J., and Slootweg, J. (2014). Method for Evaluating Smart Grid Concepts and Pilots. In *IEEE Young Res. Symp. 2014 (YRS 2014)*, pages 1–6, Ghent. EESA.

Labeeuw, W., Stragier, J., and Deconinck, G. (2015). Potential of Active Demand Reduction With Residential Wet Appliances: A Case Study for Belgium. *IEEE Trans. Smart Grid*, 6(1):315–323.

Lampropoulos, I., Kling, W. L., Ribeiro, P. F., and van den Berg, J. (2013). History of demand side management and classification of demand response control schemes. *2013 IEEE Power Energy Soc. Gen. Meet.*, pages 1–5.

Liu, W., Wu, Q., Wen, F., and Ostergaard, J. (2014). Day-Ahead Congestion Management in Distribution Systems Through Household Demand Response and Distribution Congestion Prices. *Smart Grid, IEEE Trans.*, 5(6):2739–2747.

Ma, K., Hu, G., and Spanos, C. J. (2015). A Cooperative Demand Response Scheme Using Punishment Mechanism and Application to Industrial Refrigerated Warehouses. *IEEE Trans. Ind. Informatics*, 11(6):1520–1531.

Maharashtra State Blood Transfusion Council (2014). Preservation and Storage of Blood.

Matthews, B. and Craig, I. (2013). Demand side management of a run-of-mine ore milling circuit. *Control Eng. Pract.*, 21(6):759–768.

MatWeb (2017). Unifrax Excelfrax 200 VIP Vacuum Insulation Panel.

Mitra, S., Sun, L., and Grossmann, I. E. (2013). Optimal scheduling of industrial combined heat and power plants under time-sensitive electricity prices. *Energy*, 54:194–211.

Morales González, R., Shariat Torbaghan, S., Gibescu, M., and Cobben, S. (2016). Harnessing the Flexibility of Thermostatic Loads in Microgrids with Solar Power Generation. *Energies*, 9(7):547.

Samad, T. and Kiliccote, S. (2012). Smart grid technologies and applications for the industrial sector. *Comput. Chem. Eng.*, 47:76–84.

Ton, D. and Smith, M. (2012). The U.S. Department of Energy's Microgrid Initiative. *Electr. J.*, 25(8):84–94.

Verzijlbergh, R. and Lukszo, Z. (2013). Conceptual model of a cold storage warehouse with PV generation in a smart grid setting. In *2013 10th IEEE Int. Conf. Networking, Sens. Control. ICNSC 2013*, pages 889–894, Evry. IEEE.

Wessling, F. and Blackshear, P. (1973). The Thermal Properties of Human Blood During the Freezing Process. *Heat Transf.*, 95(2):246–249.

Wilson, M. B., Luck, R., and Mago, P. J. (2015). A First-Order Study of Reduced Energy Consumption via Increased Thermal Capacitance with Thermal Storage Management in a Micro-Building. *Energies*, 8:12266–12282.

Yin, R., Kara, E. C., Li, Y., DeForest, N., Wang, K., Yong, T., and Stadler, M. (2016). Quantifying flexibility of commercial and residential loads for demand response using setpoint changes. *Appl. Energy*, 177:149–164.

Yoon, J. H., Baldick, R., and Novoselac, A. (2014). Dynamic Demand Response Controller Based on Real-Time Retail Price for Residential Buildings. *IEEE Trans. Smart Grid*, 5(1):121–129.

Zaparoli, E. L. and de Lemos, M. (1996). Simulation of Transient Response of Domestic Refrigeration Systems. In *Int. Refrig. Air Cond. Conf.*, pages 495–500, West Lafayette. Purdue University.

Zavala, V. M. (2013). Real-time optimization strategies for building systems. *Ind. Eng. Chem. Res.*, 52(9):3137–3150.